

# From phase separation to long-range order in a system of interacting electrons

Volodymyr Derzhko<sup>a</sup> and Janusz Jędrzejewski<sup>a,b,1</sup>

<sup>a</sup>*Institute of Theoretical Physics, University of Wrocław, pl. Maksa Born'a 9,  
50-204 Wrocław, Poland*

<sup>b</sup>*Department of Theoretical Physics, University of Łódź, ul. Pomorska 149/153,  
90-236 Łódź, Poland*

---

## Abstract

We study a system composed of fermions (electrons), hopping on a square lattice, and of immobile particles (ions), that is described by the spinless Falicov–Kimball Hamiltonian augmented by a next-nearest-neighbor attractive interaction between the ions (a nearest-neighbor repulsive interaction between the ions can be included and does not alter the results). A part of the grand-canonical phase diagram of this system is constructed rigorously, when the coupling between the electrons and ions is much stronger than the hopping intensity of electrons. The obtained diagram implies that, at least for a few rational densities of particles, by increasing the hopping intensity the system can be driven from a state of phase separation to a state with a long-range order. This kind of transitions occurs also, when the hopping fermions are replaced by hopping hard-core bosons.

*Key words:* Fermion lattice systems, Ground-state phase diagrams, Strongly correlated electrons, Falicov–Kimball model, Quantum phase transitions

*PACS:* 71.10.-w, 71.27.+a

---

## 1 Introduction

Since forty years, it is the Hubbard or the extended Hubbard models that are most frequently studied when properties of strongly correlated electrons are to be investigated. The central issue is the phase diagram of these models. Despite the apparent simplicity of both models and concerted efforts of

---

<sup>1</sup> Corresponding author: J. Jędrzejewski, phone: +48 71 3759415, fax: +48 71 3214454, e-mail: jjed@ift.uni.wroc.pl

many researchers, the complicated structure of these phase diagrams, even at zero temperature, has not been revealed completely and unquestionably; rigorous results are scarce. A few years ago Nakamura [1] predicted a new kind of quantum phase transition in the ground state of a half-filled extended Hubbard model chain. On a line, in the space of the two relevant interaction parameters (representing on-site and nearest-neighbor (n.n.) repulsion due to Coulomb forces, expressed in the units of the hopping intensity), for large values of these parameters, the system is in the phase-separated state, which is a mixture of a charge-density-wave phase and a spin-density-wave phase. The transition occurs when the parameters are decreased along the line, at a critical point where the parameters assume intermediate values (of the order of one). Thus, the transition region is hardly accessible by perturbation methods. A new state exhibits a long-range order, the so called bond-order-wave. There are many aspects of the phase diagram to be studied in connection with the new conjectured transition, and they are vigorously discussed in the physics literature recently [2,3,4]. In this paper we address just one aspect of the new transition that we find remarkable. Namely, by increasing the hopping intensity of electrons the system is driven from a phase-separated state to a crystalline state with a long-range order. Our aim is to construct a model of interacting electrons (by the way we consider an analogous model of interacting hard-core bosons), where the existence of a transition exhibiting this feature can be demonstrated rigorously. The model to be studied is a simplified version of the one band, spin 1/2 Hubbard model, known as the static approximation (one sort of electrons hops while the other sort is immobile), with the Hamiltonian  $H_{FK}$ , extended by a next-nearest-neighbor (n.n.n.) attractive interaction between the immobile particles, given by the Hamiltonian  $V$ . Thus the total Hamiltonian of the system reads:

$$H_0 = H_{FK} + V, \quad (1)$$

$$H_{FK} = -t \sum_{\langle x,y \rangle_1} (c_x^\dagger c_y + h.c.) + U \sum_x \left( c_x^\dagger c_x - \frac{1}{2} \right) s_x, \quad (2)$$

$$V = -\frac{\tilde{\varepsilon}}{16} \sum_{\langle x,y \rangle_2} s_x s_y, \quad t > 0, \quad \tilde{\varepsilon} > 0. \quad (3)$$

In the above formulae, the underlying lattice is a square lattice, denoted  $\Lambda$ , consisting of sites  $x, y, \dots$  whose number is  $|\Lambda|$ , having the shape of a  $\sqrt{|\Lambda|} \times \sqrt{|\Lambda|}$  torus. In (2,3) and below, the sums  $\sum_{\langle x,y \rangle_i}$ ,  $i = 1, 2, 3$ , stand for the summation over all the  $i$ -th n.n. pairs of lattice sites, with each pair counted once.

The subsystem of mobile spinless electrons is described in terms of creation and annihilation operators of an electron at site  $x$ :  $c_x^\dagger$ ,  $c_x$ , respectively, satis-

fying the canonical anticommutation relations, with  $t$  being the n.n. hopping intensity. The total electron-number operator is  $N_e = \sum_x c_x^\dagger c_x$ , and (with a little abuse of notation) the corresponding electron density is  $\rho_e = N_e/|\Lambda|$ .

The subsystem of ions is described by a collection of pseudo-spins  $\{s_x\}_{x \in \Lambda}$ , with  $s_x = 1, -1$  (1 if the site  $x$  is occupied by an ion and  $-1$  if it is empty), called the *ion configurations*. The total number of ions is  $N_i = \sum_x (s_x + 1)/2$  and the ion density is  $\rho_i = N_i/|\Lambda|$ . In contradistinction to the electron subsystem, the ions interact directly: two ions that occupy two n.n.n. sites attract each other, contributing the energy  $-\tilde{\varepsilon}/16$ , with  $\tilde{\varepsilon} > 0$ .

Clearly, in the composite system, whose Hamiltonian is given by (1), with arbitrary electron-ion coupling  $U$ , the particle-number operators  $N_e$ ,  $N_i$ , and pseudo-spins  $s_x$ , are conserved. Therefore the description of the classical subsystem in terms of the ion configurations  $S = \{s_x\}_{x \in \Lambda}$  remains valid. Whenever periodic configurations of pseudo-spins are considered it is assumed that  $\Lambda$  is sufficiently large, so that it accommodates an integer number of elementary cells.

Nowadays,  $H_{FK}$  is widely known as the Hamiltonian of the spinless Falicov–Kimball model, a simplified version of the Hamiltonian put forward in [5]. A lot of results, including rigorous ones, like a proof of the existence of a phase transition [6,7] for instance, have been obtained for the system described by this Hamiltonian (a review and an extensive list of references can be found in [8,9]).

In what follows, we shall study the ground-state phase diagram of the system defined by (1) in the grand-canonical ensemble. That is, let

$$H(\mu_e, \mu_i) = H_0 - \mu_e N_e - \mu_i N_i, \quad (4)$$

where  $\mu_e, \mu_i$  are the chemical potentials of the electrons and ions, respectively, and let  $E_S(\mu_e, \mu_i)$  be the ground-state energy of  $H(\mu_e, \mu_i)$ , for a given configuration  $S$  of the ions. Then, the ground-state energy of  $H(\mu_e, \mu_i)$ ,  $E_G(\mu_e, \mu_i)$ , is defined as  $E_G(\mu_e, \mu_i) = \min \{E_S(\mu_e, \mu_i) : S\}$ . The minimum is attained at the set  $G$  of the ground-state configurations of ions. We shall determine the subsets of the  $(\mu_e, \mu_i)$ -plane, where  $G$  consists of periodic configurations of ions, uniformly in the size of the underlying square lattice.

The paper is organized as follows. In the first subsection of the next section we provide a number of symmetry properties of the ground-state energy,  $E_S(\mu_e, \mu_i)$ , which facilitate the studies of the phase diagram that follow, and give the strong-coupling expansion of  $E_S(\mu_e, \mu_i)$  in the case of hopping fermions (subsection 2.1). Then, in subsection 2.2 we construct the grand-canonical phase diagram due to the ground-state energy truncated at fourth order of the strong-coupling expansion in the case of hopping fermions (this is

sufficient to draw our conclusions). After that, in subsection 2.3 we consider the grand-canonical phase diagram due to the ground-state energy truncated at fourth order of the strong-coupling expansion in the case of hopping hard-core bosons. Finally, in Section 3 we discuss the implications of the phase diagram obtained with the truncated effective interaction, when the remainder of the strong-coupling expansion is taken into account.

## 2 Grand-canonical phase diagram in the strong coupling regime

### 2.1 Properties of $E_S(\mu_e, \mu_i)$ and its strong-coupling expansion

In studies of grand-canonical phase diagrams an important role is played by unitary transformations that exchange particles and holes:  $c_x^+ c_x \rightarrow 1 - c_x^+ c_x$  and  $s_x \rightarrow -s_x$ , and for some  $(\mu_e^0, \mu_i^0)$  leave the Hamiltonian  $H(\mu_e, \mu_i)$  invariant. For the electron subsystem such a role is played by the transformations:  $c_x^+ \rightarrow \epsilon_x c_x$ , with  $\epsilon_x = 1$  at the even sublattice of  $\Lambda$  and  $\epsilon_x = -1$  at the odd one. Clearly, since  $H_0$  is invariant under the joint hole-particle transformation of electrons and ions,  $H(\mu_e, \mu_i)$  is hole-particle invariant at the point  $(0, 0)$ . At the hole-particle symmetry point, the system under consideration has very special properties, which simplify studies of its phase diagram [7]. Moreover, by means of the defined above hole-particle transformations one can determine a number of symmetries of the grand-canonical phase diagram [10]. The peculiarity of the model is that the case of attraction ( $U < 0$ ) and the case of repulsion ( $U > 0$ ) are related by a unitary transformation (the hole-particle transformation for ions): if  $S$  is a ground-state configuration at  $(\mu_e, \mu_i)$  for  $U > 0$ , then  $-S$  is the ground-state configuration at  $(\mu_e, -\mu_i)$  for  $U < 0$ . Consequently, without any loss of generality one can fix the sign of the coupling constant  $U$ . Moreover (with the sign of  $U$  fixed), there is the *inversion symmetry* of the grand-canonical phase diagram, that is, if  $S$  is a ground-state configuration at  $(\mu_e, \mu_i)$ , then  $-S$  is the ground-state configuration at  $(-\mu_e, -\mu_i)$ . Therefore, it is enough to determine the phase diagram in the half-plane specified by fixing the sign of one of the chemical potentials. Additional properties emerge in the *strong-coupling regime*, i.e. for  $|U| > 4t$  [10]. Specifically, if the electron chemical potential is in the open interval  $|\mu_e| < |U| - 4t$ , then for any two ion configurations  $S, S'$  the energy difference  $E_S(\mu_e, \mu_i) - E_{S'}(\mu_e, \mu_i)$  is constant along the lines  $\mu_e \pm \mu_i = \text{const}$ , with minus sign referring to the case of positive  $U$  (repulsion) while the plus sign — to the case of negative  $U$  (attraction). This property together with the inversion symmetry implies that in the stripe  $|\mu_e| < |U| - 4t$  of the  $(\mu_e, \mu_i)$ -plane it is enough to determine the phase diagram at the half-line  $\mu_e = 0, \mu_i < 0$  (or  $\mu_i > 0$ ).

Our aim in this paper is to investigate the ground-state phase diagram off the symmetry point. According to the state of the art, this is feasible only in the strong-coupling regime. From now on, we shall consider exclusively the case of the strong positive coupling, i.e.  $U/t > 4$ . In this case, it is convenient to express all the parameters of  $H(\mu_e, \mu_i)$ , in the units of  $|U|$ , i.e. we change  $t \rightarrow t/|U|$ ,  $\tilde{\varepsilon} \rightarrow \tilde{\varepsilon}/|U|$ , etc, but keep the previous notation. Then,  $H_0$  assumes the form

$$H_0 = -t \sum_{\langle x,y \rangle_1} (c_x^\dagger c_y + h.c.) + 1 \sum_x \left( c_x^\dagger c_x - \frac{1}{2} \right) s_x - \frac{\tilde{\varepsilon}}{16} \sum_{\langle x,y \rangle_2} s_x s_y, \quad (5)$$

and the strong-coupling regime is given by the condition  $t < 1/4$ . The possibility of studying the phase diagram in the strong-coupling regime stems from the fact that in the open stripe  $|\mu_e| < 1 - 4t$ , the ion density  $\rho_i$  of a ground-state configuration determines the electron density:  $\rho_e = \rho_i$  for  $U < 0$ , and  $\rho_e = 1 - \rho_i$  for  $U > 0$ . Then, one can formally expand the ground-state energy  $E_S(\mu_e, \mu_i)$  in powers of  $t$ , what results in the so called effective Hamiltonian:

$$\begin{aligned} E_S(\mu_e, \mu_i) = & -\frac{1}{2}(\mu_i - \mu_e) \sum_x s_x - \frac{1}{2}(\mu_i + \mu_e + 1) |\Lambda| + \\ & \left[ \frac{t^2}{4} - \frac{9t^4}{16} \right] \sum_{\langle x,y \rangle_1} s_x s_y + \left[ \frac{3t^4}{16} - \frac{\tilde{\varepsilon}}{16} \right] \sum_{\langle x,y \rangle_2} s_x s_y + \\ & \frac{t^4}{8} \sum_{\langle x,y \rangle_3} s_x s_y + \frac{t^4}{16} \sum_P (1 + 5s_P) + R^{(4)}, \end{aligned} \quad (6)$$

up to a term independent of the ion configuration and the chemical potentials. In (6),  $P$  denotes the  $(2 \times 2)$ -plaquette of the square lattice  $\Lambda$ ,  $s_P$  stands for the product of pseudo-spins assigned to the corners of  $P$ , and the remainder  $R^{(4)}$ , which is independent of the chemical potentials and  $\tilde{\varepsilon}$ , collects those terms of the expansion that are proportional to  $t^{2m}$ , with  $m = 3, 4, \dots$ . The expansion (6) (with  $\tilde{\varepsilon} = 0$ ) was introduced and the phase diagram, according to the expansion truncated at the fourth order, was studied in [10]. It turns out however that, in the strong-coupling regime the expansion (6) is absolutely convergent, uniformly in  $\Lambda$  [11,12]. Due to this fact, it is possible to establish rigorously a part of the phase diagram (that is the ground states are determined everywhere in the  $(\mu_e, \mu_i)$ -plane, except some regions), by determining the phase diagram of the expansion truncated at the order  $k$ , that is according to the effective Hamiltonian  $E_S^{(k)}(\mu_e, \mu_i)$ .

## 2.2 Construction of the phase diagram up to fourth order. The case of hopping fermions

To construct the phase diagram according to the effective Hamiltonian  $E_S^{(k)}(\mu_e, \mu_i)$ , we use the  $m$ -potential method introduced in [13], with technical developments given in [10,11,12]. By virtue of the comments in the preceding subsection, in what follows we set  $\mu_e = 0$  and  $\mu_i = \mu$ . In the order zero the effective Hamiltonian reads:

$$\begin{aligned} E_S^{(0)}(0, \mu) &= -\frac{\mu}{2} \sum_x (s_x + 1) - \frac{\tilde{\varepsilon}}{16} \sum_{\langle x, y \rangle_2} s_x s_y \\ &= \sum_P H_P^{(0)}, \end{aligned} \quad (7)$$

where

$$H_P^{(0)} = -\frac{\mu}{8} \sum_x (s_x + 1) - \frac{\tilde{\varepsilon}}{16} \sum_{\langle x, y \rangle_2} s_x s_y. \quad (8)$$

Except the point  $\mu = 0, \tilde{\varepsilon} = 0$ , where all the configurations have the same energy, the plaquette potentials  $H_P^{(0)}$  are minimized by the restrictions to  $P$  of a few periodic configurations on  $\Lambda$ . For  $\mu < 0$  ( $\mu > 0$ ) it is the *ferromagnetic configuration*  $S_-$  ( $S_+$ ), where  $s_x = -1$  at every site ( $s_x = +1$  at every site), while at the half-line  $\mu = 0, \tilde{\varepsilon} > 0$ , besides the ferromagnetic configurations  $S_-$  and  $S_+$ , these are the two *antiferromagnetic (or chessboard) configurations*  $S_{cb}^e$ , where  $s_x = \epsilon_x$ , and  $S_{cb}^o$ , where  $s_x = -\epsilon_x$ , with  $\epsilon_x = 1$  if  $x$  belongs to the even sublattice of  $\Lambda$  and  $\epsilon_x = -1$  otherwise. Moreover, out of the restrictions  $S_{-|P}$ ,  $S_{+|P}$ ,  $S_{cb|P}^e$ , and  $S_{cb|P}^o$  only four ground-state configurations can be built, which coincide with the four configurations named above. Clearly, this is due to the n.n.n. ferromagnetic interaction. The phase diagram according to the effective Hamiltonian  $E_S^{(0)}(0, \mu)$  is shown in Fig. 1.

In the next order, which takes into the account interactions proportional to  $t^2$ , a n.n. antiferromagnetic interaction appears. The effective Hamiltonian reads

$$\begin{aligned} E_S^{(2)}(0, \mu) &= -\frac{\mu}{2} \sum_x (s_x + 1) + \frac{t^2}{4} \sum_{\langle x, y \rangle_1} s_x s_y - \frac{\tilde{\varepsilon}}{16} \sum_{\langle x, y \rangle_2} s_x s_y \\ &= \sum_P H_P^{(2)}, \end{aligned} \quad (9)$$

where,

$$H_P^{(2)} = -\frac{\mu}{8} \sum_x (s_x + 1) + \frac{t^2}{8} \sum_{\langle x, y \rangle_1} s_x s_y - \frac{\tilde{\varepsilon}}{16} \sum_{\langle x, y \rangle_2} s_x s_y. \quad (10)$$

By determining the plaquette configurations that minimize the potentials  $H_P^{(2)}$  one finds the ground-state phase diagram shown in Fig. 2. The boundary

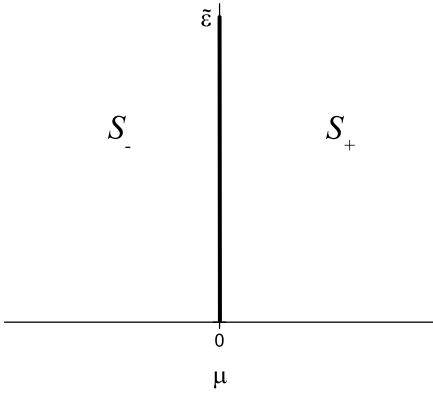


Fig. 1. Ground-state phase diagram of  $E_S^{(0)}(0, \mu)$ .

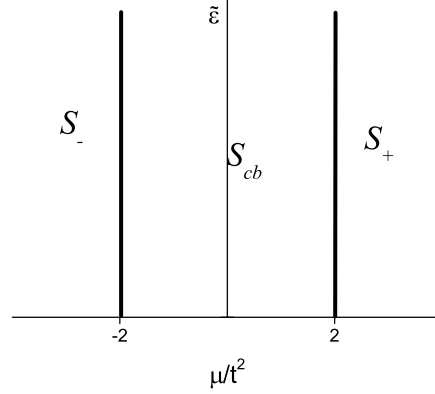


Fig. 2. Ground-state phase diagram of  $E_S^{(2)}(0, \mu)$ .

between  $S_+$  and  $S_-$ , determined in the order zero, i.e. the half-line  $\mu = 0$ ,  $\tilde{\varepsilon} > 0$ , is replaced by the stripe of the width  $4t^2$ , centered at this half-line. Outside this stripe the ground state remains ferromagnetic. Inside the stripe, including its boundary on the line  $\tilde{\varepsilon} = 0$ , there are only two ground-state configurations, the antiferromagnetic ones. At the boundary of the stripe, given by  $\mu = -2t^2, \tilde{\varepsilon} > 0$  ( $\mu = 2t^2, \tilde{\varepsilon} > 0$ ), there are exactly three ground-state configurations  $S_-$ ,  $S_{cb}^e$ , and  $S_{cb}^o$  ( $S_+$ ,  $S_{cb}^e$ , and  $S_{cb}^o$ ). Only at the points  $(\mu = \pm 2t^2, \tilde{\varepsilon} = 0)$  the number of ground-state configurations grows exponentially with the size of the underlying lattice (like  $\exp(\text{const}|\Lambda|)$ ). The Hamiltonian  $E_S^{(2)}(0, \mu)$  is known in the physics literature as the Fisher-stabilized Ising antiferromagnet [14].

To proceed further and analyze the effect of the fourth-order interactions, we make use of the inversion symmetry that enables us to fix, without any loss of generality, the sign of the chemical potential. From now on, we restrict our investigations to the case  $\mu < 0$ .

Let us emphasize that we are interested in the phase diagram for sufficiently small  $t$ . Therefore clearly, it is the neighborhood of radius  $O(t^4)$  of the point  $\mu = \pm 2t^2, \tilde{\varepsilon} = 0$ , in the  $(\mu, \tilde{\varepsilon})$ -plane, where the effect of the fourth order interactions can be most significant. In this neighborhood, it is convenient to introduce the new coordinates,  $\delta, \varepsilon$ , as follows:

$$\mu = -2t^2 + \delta t^4, \quad \tilde{\varepsilon} = \varepsilon t^4. \quad (11)$$

In terms of  $\delta, \varepsilon$ , the effective Hamiltonian up to the order four can be written in the form:

$$E_S^{(4)}(0, \delta) = \frac{t^2}{4} \sum_{\langle x, y \rangle_1} (s_x s_y + s_x + s_y + 1) + \frac{t^4}{2} \sum_T H_T^{(4)} = \quad (12)$$

$$t^2 \sum_{\substack{\langle x, y \rangle_1 \\ s_x = s_y = 1}} 1 + \frac{t^4}{2} H_{\text{eff}}^{(4)},$$

with

$$H_T^{(4)} = -\delta (s_5 + 1) - \frac{3}{16} \sum_{\langle x, y \rangle_1} s_x s_y + \left[ \frac{3}{32} - \frac{\varepsilon}{32} \right] \sum_{\langle x, y \rangle_2} s_x s_y + \quad (13)$$

$$\frac{1}{12} \sum_{\langle x, y \rangle_3} s_x s_y + \frac{1}{32} \sum_P (5s_P + 1),$$

where we have omitted the term  $t^2|\Lambda|/2$ . In (12,13),  $T$  stands for a  $(3 \times 3)$ -plaquette (later on called the  $T$ -plaquette) of the square lattice, whose sites are labeled from the left to the right, starting at the bottom left corner, so that  $s_5$  is the pseudo-spin of the central site and its left-neighbor pseudo-spin is  $s_4$ . The above form of  $E_S^{(4)}(0, \delta)$  shows manifestly that, in a neighborhood of the point  $\delta = 0$ ,  $\varepsilon = 0$  whose radius is  $O(1)$ , those configurations that contain pairs of n.n. sites,  $\langle x, y \rangle_1$ , with pseudo-spins  $s_x = s_y = 1$  cannot be the ground state configurations (their energy is larger than the energy of the configurations that do not contain such pairs by a large energy of the order  $O(t^2)$ ). Therefore, in the considered region of the phase diagram, all the effects due to the interactions up to fourth order are described by the effective Hamiltonian  $H_{\text{eff}}^{(4)}$ , and the only admissible configurations are those that do not contain any pairs of n.n. sites with pseudo-spins taking the value 1.

To determine the phase diagram due to  $H_{\text{eff}}^{(4)}$  we use, as before, the  $m$ -potential method. However, in contrast to the lower-order cases the analysis is not that straightforward. The potentials  $H_T^{(4)}$  cannot serve as the  $m$ -potentials in the whole  $(\delta, \varepsilon)$ -plane. This difficulty can be overcome by introducing the so called zero-potentials [10,11,12]. Here, we follow closely [11,12] and introduce the zero-potentials  $K_T^{(4)}$  such that they are invariant with respect to the symmetries of  $H_0$  and satisfy the condition

$$\sum_T K_T^{(4)} = 0. \quad (14)$$

Moreover, the zero-potentials  $K_T^{(4)}$  are chosen in the following form

$$K_T^{(4)} = \sum_{i=1}^5 \alpha_i k_T^{(i)}, \quad (15)$$

where  $\alpha_i$  are real linear functions of  $\delta$  and  $\varepsilon$  (to be determined in the process of constructing the phase diagram), while the potentials  $k_T^{(i)}$  are given by



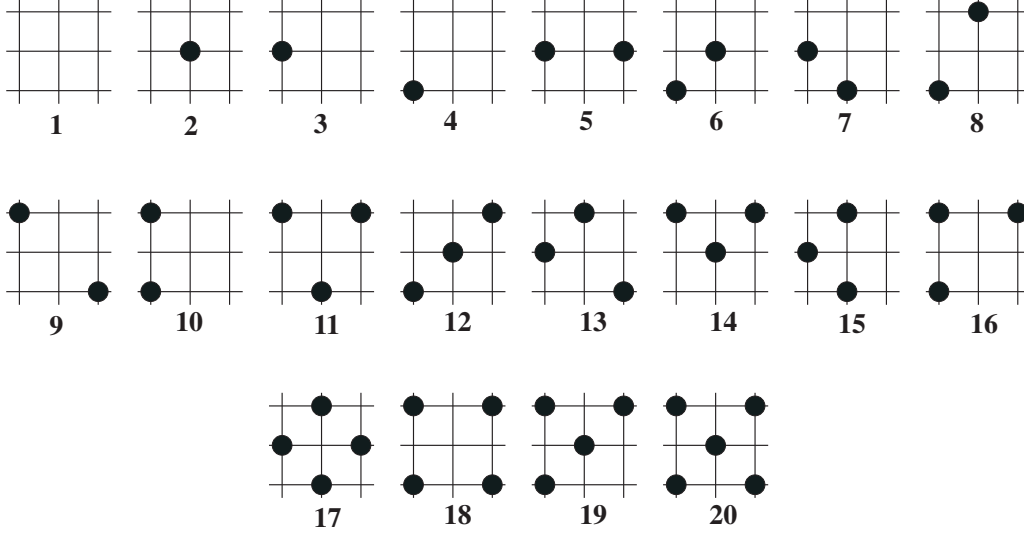


Fig. 3. All the admissible  $T$ -plaquette configurations (up to symmetries).

$$\begin{aligned}
k_T^{(1)} &= s_1 + s_3 + s_7 + s_9 - 4s_5, \\
k_T^{(2)} &= s_2 + s_4 + s_6 + s_8 - 4s_5, \\
k_T^{(3)} &= s_1s_2 + s_2s_3 + s_3s_6 + s_6s_9 + s_8s_9 + s_7s_8 + s_4s_7 + s_1s_4 \\
&\quad - 2s_2s_5 - 2s_5s_6 - 2s_5s_8 - 2s_4s_5, \\
k_T^{(4)} &= s_1s_5 + s_3s_5 + s_5s_9 + s_5s_7 - s_2s_4 - s_4s_8 - s_8s_6 - s_2s_6, \\
k_T^{(5)} &= s_1s_3 + s_3s_9 + s_7s_9 + s_1s_7 - 2s_4s_6 - 2s_2s_8.
\end{aligned} \tag{16}$$

We note that the potentials  $k_T^{(i)}$  are invariant with respect to the symmetries of the Hamiltonian  $H_0$  and they satisfy the condition (14). Consequently, the same properties are shared by the potentials  $K_T^{(4)}$ . Now, we can rewrite  $H_{\text{eff}}^{(4)}$  as follows

$$H_{\text{eff}}^{(4)} = \sum_T (H_T^{(4)} + K_T^{(4)}), \tag{17}$$

and the problem is to find, at each point  $(\delta, \varepsilon)$ , the  $T$ -plaquette configurations that minimize the potential  $H_T^{(4)} + K_T^{(4)}$ . Taking into account the symmetries of the Hamiltonian, there are 20 *admissible  $T$ -plaquette configurations* whose energies have to be compared. These configurations are displayed and labelled (as in [11]) in Fig. 3. The explicit analysis shows that the  $(\delta, \varepsilon)$ -plane decomposes into five open domains  $\mathcal{S}_-$ ,  $\mathcal{S}_{cb}$ ,  $\mathcal{S}_1$ ,  $\mathcal{S}_2$ , and  $\mathcal{S}_3$ , whose boundaries consist of straight-line segments, see Fig. 4. We shall adopt the same symbols to denote also the sets of ground-state configurations in these domains. In each point  $(\delta, \varepsilon)$  of a domain, it is possible to choose the values of the coefficients  $\alpha_i$  such that the set of  $T$ -plaquette configurations minimizing the potential  $H_T^{(4)} + K_T^{(4)}$ , denoted  $\mathcal{S}_{cb|T}$ , etc., is the same. Remarkably, out of these minimizing  $T$ -plaquette configurations (in a domain) one can construct exactly one, up to the symmetries of  $H_0$ , ground-state configuration on the lattice  $\Lambda$ .

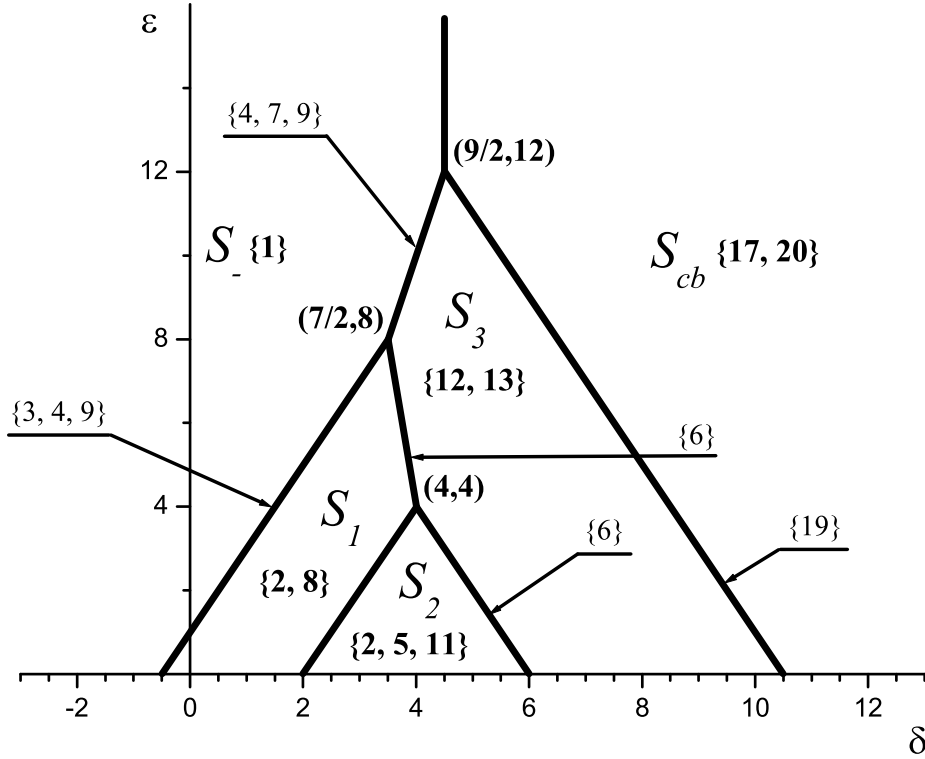


Fig. 4. Ground-state phase diagram of  $H_{\text{eff}}^{(4)}$ . By the crossing points of boundary-line segments we give their coordinates. The numbers in curly brackets, displayed by the arrows pointing towards the boundary-line segments, identify the additional minimizing  $T$ -plaquette configurations. For more comments see the text.

The obtained configurations turn out to be periodic. Specifically, one finds that the minimizing  $T$ -plaquette configurations are:  $\mathcal{S}_{-|T} = \{1\}$ ,  $\mathcal{S}_{cb|T} = \{17, 20\}$ ,  $\mathcal{S}_{1|T} = \{2, 8\}$ ,  $\mathcal{S}_{2|T} = \{2, 5, 11\}$ , and  $\mathcal{S}_{3|T} = \{12, 13\}$ , where the numbers in the curly brackets stand for the labels, according to Fig. 3, of the minimizing  $T$ -plaquette configurations, and the  $T$ -plaquette configurations that can be obtained from the named ones, by applying symmetries of  $H_0$ , are omitted. Consequently, the sets of ground-state configurations in the five open domains are given by:  $\mathcal{S}_{-} = \{\mathcal{S}_{-}\}$ ,  $\mathcal{S}_{cb} = \{\mathcal{S}_{cb}^e, \mathcal{S}_{cb}^o\}$ ,  $\mathcal{S}_1 = \{\mathcal{S}_1^j\}_{j=1}^{j=10}$ ,  $\mathcal{S}_2 = \{\mathcal{S}_2^j\}_{j=1}^{j=8}$ , and  $\mathcal{S}_3 = \{\mathcal{S}_3^j\}_{j=1}^{j=6}$ , where the representative configurations of  $\mathcal{S}_{cb}$ ,  $\mathcal{S}_1$ ,  $\mathcal{S}_2$ , and  $\mathcal{S}_3$ , are displayed in Fig. 5. The coefficients  $\alpha_i$  are given in the Table 1 included in Appendix.

For  $\varepsilon = 0$  the obtained phase diagram coincides with the phase diagram of the spinless Falicov–Kimball model [10,12]. If  $\varepsilon < 12$ , when  $\delta$  is increased, it crosses some “critical” values,  $\delta_{cr}(\varepsilon)$ , that limit the  $\delta$ -extent of the domains  $\mathcal{S}_{-}$ ,  $\mathcal{S}_1$ ,  $\mathcal{S}_2$ ,  $\mathcal{S}_3$ , and  $\mathcal{S}_{cb}$ . In particular,  $\delta_{cr}(0) = -1/2, 2, 6, 21/2$ , respectively.

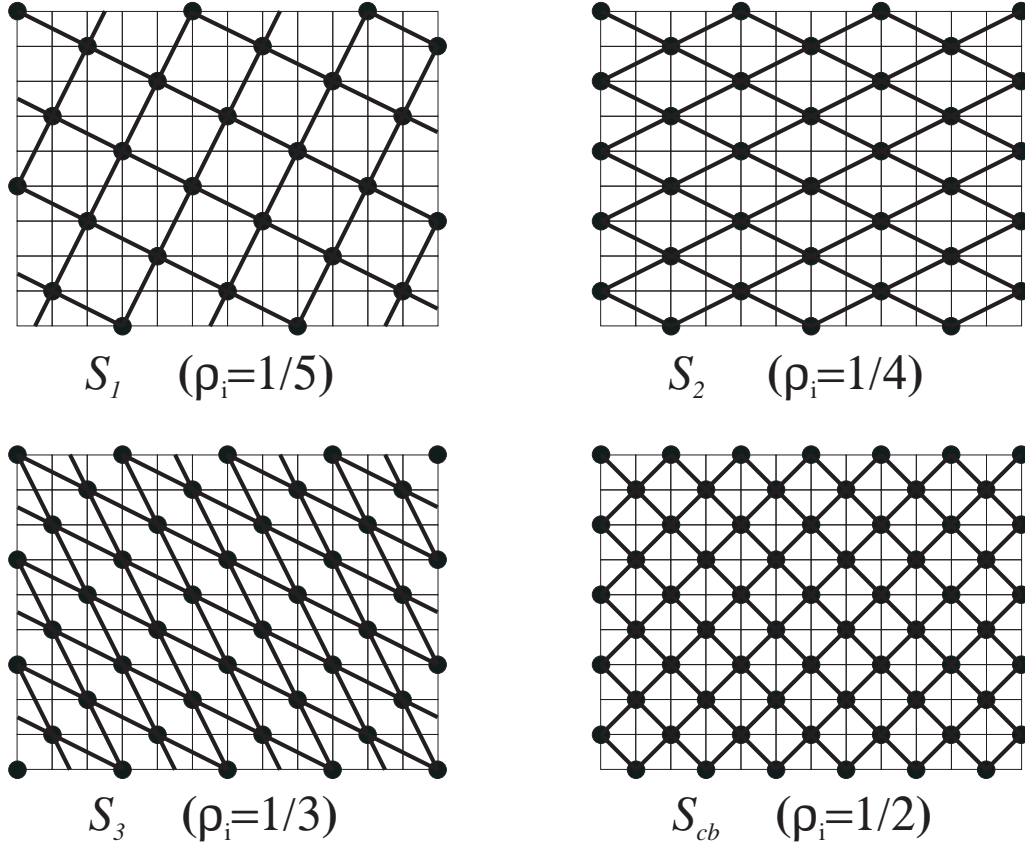


Fig. 5. Ground-state configurations, which appear for  $\mu < 0$ .

Similarly, as  $\varepsilon$  is increased, it passes through three “critical” values  $\varepsilon_{cr} = 4, 8, 12$ , that limit the  $\varepsilon$ -extent of the domains  $\mathcal{S}_2, \mathcal{S}_1, \mathcal{S}_3$ , respectively. Thus, there is no  $\mathcal{S}_2$  ground-state configurations for  $\varepsilon > 4$ , etc. Above  $\varepsilon = 12$  the phase diagram is independent of  $\varepsilon$ .

At the boundaries of the domains the situation is more involved. Let  $\mathcal{S}, \mathcal{S}'$  be two domains of the considered phase diagram. The set of the minimizing  $T$ -plaquette configurations at the boundary between  $\mathcal{S}$  and  $\mathcal{S}'$  consists always of  $\mathcal{S}_{|T} \cup \mathcal{S}'_{|T}$ , but it may contain also some additional  $T$ -plaquette configurations of minimal energy. If it is the case, a great many of ground-state configurations exists at the boundary. Except the boundary between  $\mathcal{S}_-$  and  $\mathcal{S}_{cb}$ , the number of ground-state configurations that can be built out of the minimizing  $T$ -plaquette configurations grows indefinitely with the size of the lattice.

Specifically, at the boundary between  $\mathcal{S}_-$  and  $\mathcal{S}_{cb}$  the set of the minimizing  $T$ -plaquette configurations is  $\mathcal{S}_{-|T} \cup \mathcal{S}_{cb|T}$ . Clearly, only the three periodic configurations,  $\mathcal{S}_-, \mathcal{S}_{cb}^e$ , and  $\mathcal{S}_{cb}^o$ , can be built out of them.

Then, at the boundary between  $\mathcal{S}_-$  and  $\mathcal{S}_3$  the set of the minimizing  $T$ -plaquette configurations is  $\mathcal{S}_{-|T} \cup \mathcal{S}_{3|T} \cup \{4, 7, 9\}$ . A simple reasoning shows that

in any ground-state configuration all the lattice lines with one of the slopes 1 or  $-1$  are ordered ferromagnetically. On any horizontal line of sites, every two consecutive sites with pseudo-spins 1 are separated by at least two sites with pseudo-spins  $-1$ . That is, the ground-state configurations at the boundary “interpolate” between the configurations  $\mathcal{S}_3$  and  $\mathcal{S}_-$ . The number of such configurations grows as  $\exp(\text{const}\sqrt{|\Lambda|})$ . The last segment of the boundary of  $\mathcal{S}_-$  is the boundary between  $\mathcal{S}_-$  and  $\mathcal{S}_1$ . The set of the minimizing  $T$ -plaquette configurations is  $\mathcal{S}_{-|T} \cup \mathcal{S}_{1|T} \cup \{3, 4, 9\}$ . Therefore, flipping in  $\mathcal{S}_1$  any set of pseudo-spins 1, we obtain a ground-state configuration. Their number grows as  $\exp(\text{const}|\Lambda|)$ .

The situation at the boundary between  $\mathcal{S}_1$  and  $\mathcal{S}_3$  is more intricate. The set of the minimizing  $T$ -plaquette configurations is  $\mathcal{S}_{1|T} \cup \mathcal{S}_{3|T} \cup \{6\}$ . In any ground-state configuration the lattice lines with one of the slopes 2,  $1/2$ ,  $-2$ , or  $-1/2$  are ordered ferromagnetically. Along such a line, it is possible to build a stratum, of any width, that consists of elementary cells of  $\mathcal{S}_1$  kind ( $\sqrt{5} \times \sqrt{5}$  squares) (see Fig. 5), then a stratum that consists of elementary cells of  $\mathcal{S}_3$  kind (diamonds), and so on. The number of such periodic configurations grows as  $\exp(\text{const}\sqrt{|\Lambda|})$ . Moreover, it is possible to build quasi-periodic tilings composed of square elementary cells and diamonds [15].

The three boundaries that remain to be described, have already been discussed in the literature. At the boundary between  $\mathcal{S}_3$  and  $\mathcal{S}_{cb}$ , the set of the minimizing  $T$ -plaquette configurations is  $\mathcal{S}_{3|T} \cup \mathcal{S}_{cb|T} \cup \{19\}$ . In any ground-state configuration the lattice lines with slope 1 or  $-1$  are ordered ferromagnetically. On every horizontal and every vertical line of sites, any two consecutive sites with pseudo-spins 1 are separated by either one or two sites with pseudo-spins equal to  $-1$  [11]. Thus, the number of such configurations grows as  $\exp(\text{const}\sqrt{|\Lambda|})$ .

Next, at the boundary between  $\mathcal{S}_2$  and  $\mathcal{S}_3$  the set of the minimizing  $T$ -plaquette configurations is  $\mathcal{S}_{2|T} \cup \mathcal{S}_{3|T} \cup \{6\}$ . In any ground-state configuration the lattice lines with one of the slopes 2,  $1/2$ ,  $-2$ , or  $-1/2$  are ordered ferromagnetically. If the slope is  $\pm 2$ , on every vertical line of sites, any two consecutive sites with pseudo-spins 1 are separated by either two or three sites with pseudo-spins  $-1$ . If the slope is  $\pm 1/2$ , on every horizontal line any two consecutive sites with pseudo-spins 1 are separated by either two or three sites with pseudo-spins  $-1$  [11]. The number of such configurations grows as  $\exp(\text{const}\sqrt{|\Lambda|})$ .

Finally at the boundary between  $\mathcal{S}_1$  and  $\mathcal{S}_2$ , the set of the minimizing  $T$ -plaquette configurations is  $\mathcal{S}_{1|T} \cup \mathcal{S}_{2|T}$ . Here the situation is analogous to that of the boundary between  $\mathcal{S}_1$  and  $\mathcal{S}_3$  [15].

### 2.3 Construction of the phase diagram up to fourth order. The case of hopping hard-core bosons

In the case of hard-core bosons, the creation and annihilation operators at site  $x$ :  $c_x^+$ ,  $c_x$ , respectively, satisfy the anticommutation relations, as fermions, but in contrast to fermions they commute at different sites. Consequently, with the system of hard-core bosons, described by the Hamiltonian (5), we cannot associate a one-particle Hamiltonian and derive the small  $t$  effective interaction as in the case of fermions. The effective interaction up to fourth order has been derived in [12] by means of a closed-loop expansion, and reads:

$$\begin{aligned} \tilde{E}_S(\mu_e, \mu_i) = & -\frac{1}{2}(\mu_i - \mu_e) \sum_x s_x - \frac{1}{2}(\mu_i + \mu_e + 1) |\Lambda| + \\ & \left[ \frac{t^2}{4} - \frac{5t^4}{16} \right] \sum_{\langle x,y \rangle_1} s_x s_y + \left[ \frac{5t^4}{16} - \frac{\tilde{\varepsilon}}{16} \right] \sum_{\langle x,y \rangle_2} s_x s_y + \\ & \frac{t^4}{8} \sum_{\langle x,y \rangle_3} s_x s_y - \frac{t^4}{16} \sum_P (5 + s_P) + \tilde{R}^{(4)}. \end{aligned} \quad (18)$$

The above expansion is convergent absolutely if  $t < 1/16$  and  $|\mu_e| < 1 - 16t$ . The latter condition implies that  $N_e + N_i = |\Lambda|$ . Setting in (18)  $\mu_e = 0$ ,  $\mu_i = -2t^2 + \delta t^4$ , and dropping the remainder  $\tilde{R}^{(4)}$ , we get the effective interaction up to fourth order,  $\tilde{E}_S^{(4)}(0, \delta)$ , and the effective Hamiltonian,  $\tilde{H}_{\text{eff}}^{(4)}$ , defined as in (12). Then, repeating all the steps of the construction of the phase diagram up to fourth order, carried out for fermions in the previous section, leads to the phase diagram displayed in Fig. 6. The diagram in Fig. 6 is described in the same way as the diagram in Fig. 4. If the phase diagram due to  $\tilde{E}_S^{(4)}(0, \delta)$  is limited to positive  $\varepsilon$ , then it differs significantly from its counterpart for fermions, the  $\mathcal{S}_2$ -domain is missing. But the analysis extended to negative values of  $\varepsilon$  reveals the  $\mathcal{S}_2$ -domain, and shows that the phase diagram of hard-core bosons, limited to  $\varepsilon \geq -4$ , after translating by the vector  $(2, 4)$  becomes identical with the phase diagram of fermions, limited to  $\varepsilon \geq 0$ .

### 3 Discussion of the phase diagram and summary

The ground-state phases of the whole electron-ion system under consideration can be distinguished by their ground-state arrangements of ions. Thus, we can speak of  $\mathcal{S}_{cb}$ -phase, where the arrangement of the ions is given by the chess-board configurations, etc. Let us ignore for the moment the remainder  $R^{(4)}$  in the expansion (6). Then, it follows from the grand-canonical phase diagram due to the effective interaction truncated at fourth order that if  $\rho_i = \rho_e = 1/2$ ,

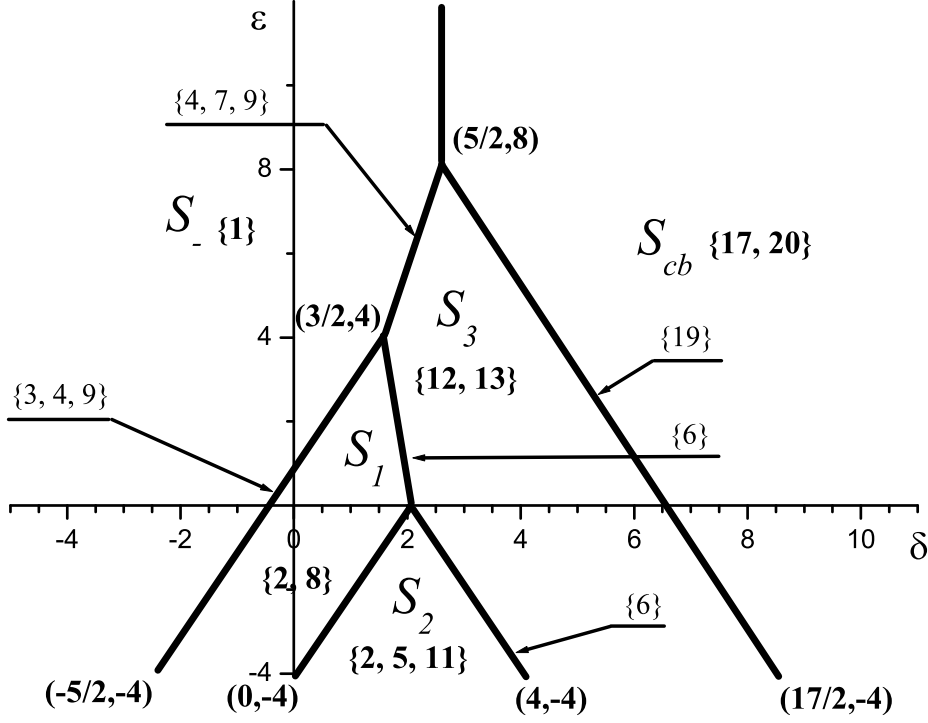


Fig. 6. Ground-state phase diagram of  $\tilde{H}_{\text{eff}}^{(4)}$ . See description of Fig. 4.

then the ground-state phase is the  $\mathcal{S}_{cb}$ -phase. More generally, consider a sequence of rational ion densities  $\rho_i = 0, 1/5, 1/4, 1/3, 1/2$  (and the corresponding electron densities  $\rho_e = 1 - \rho_i$ ). Then, for some densities of this sequence, depending on  $\varepsilon$ , the ground-state phases of the system are characterized by crystalline, i.e. exhibiting positional long-range order, arrangements of the ions, given by the ion configurations  $\mathcal{S}_-, \mathcal{S}_1, \mathcal{S}_2, \mathcal{S}_3$  and  $\mathcal{S}_{cb}$ , of the corresponding density. For  $\varepsilon > 12$ , we can have only two crystalline phases:  $\mathcal{S}_-$ -phase and  $\mathcal{S}_{cb}$ -phase. At the half-line, given by  $\delta = 9/2$  and  $\varepsilon > 12$ , these two phases and only these two ones coexist, i.e. any  $S$  that is not in  $\mathcal{S}_- \cup \mathcal{S}_{cb}$  has higher energy. Since,

$$\begin{aligned}
 & E_S^{(4)} \left( 0, \frac{9}{2} \right) + t^4 \left( \frac{\varepsilon}{8} + \frac{11}{64} \right) |\Lambda| = \\
 & \frac{t^4}{2} H_{\text{eff}}^{(4)} + t^2 \sum_{\substack{\langle x, y \rangle_1 \\ s_x = s_y = 1}} 1 + t^4 \left( \frac{\varepsilon}{8} + \frac{11}{64} \right) |\Lambda| = \\
 & \frac{t^4}{2} \sum_T \left( H_T^{(4)} + K_T^{(4)} - E_T^{(-, cb)} \right) + t^2 \sum_{\substack{\langle x, y \rangle_1 \\ s_x = s_y = 1}} 1, \tag{19}
 \end{aligned}$$

where  $H_{\text{eff}}^{(4)}$ ,  $H_T^{(4)}$ , and  $K_T^{(4)}$  are evaluated at  $\delta = 9/2$ , and  $E_T^{(-,cb)}$  stands for the common value of  $H_T^{(4)} + K_T^{(4)}$  obtained for  $S \in \mathcal{S}_- \cup \mathcal{S}_{cb}$  and  $\delta = 9/2$ , the coexistence of  $\mathcal{S}_-$ -phase and  $\mathcal{S}_{cb}$ -phase follows from the following inequality:

$$\begin{aligned} & \frac{t^4}{64}(\varepsilon - 12) |\mathcal{T}_{-,cb}(S)| \leq \\ & \frac{t^4}{2} \sum_T \left( H_T^{(4)} + K_T^{(4)} - E_T^{(-,cb)} \right) + t^2 \sum_{\substack{\langle x,y \rangle_1 \\ s_x = s_y = 1}} 1 \leq \\ & \mathcal{C}^{(4)} t^2 |\mathcal{T}_{-,cb}(S)|, \end{aligned} \quad (20)$$

for any configuration  $S$  and  $\varepsilon > 12$ . In (20),  $H_T^{(4)}$  and  $K_T^{(4)}$  are also evaluated at  $\delta = 9/2$ ,  $\mathcal{T}_{-,cb}(S)$  stands for the set of the  $T$ -plaquettes such that  $S|_T$  does not coincide with  $T$ -plaquette configurations labelled by 1, 17, 20 (we call  $\mathcal{T}_{-,cb}(S)$  the set of *T-plaquette excitations* relative to the configurations in  $\mathcal{S}_- \cup \mathcal{S}_{cb}$ ),  $|\mathcal{T}_{-,cb}(S)|$  is the cardinality of  $\mathcal{T}_{-,cb}(S)$ , and  $\mathcal{C}^{(4)}$  is a constant (i.e.  $\mathcal{C}^{(4)}$  is independent of  $S$ ,  $t$ ,  $\varepsilon$ , and  $\Lambda$ ). The inequality (20), together with the variational argument constructed in [16], can be used to prove that for any density  $0 < \rho_i < 1/2$ , the ground-state phase is a mixture (a state of phase separation) of the  $\mathcal{S}_-$ -phase and  $\mathcal{S}_{cb}$ -phase. Specifically, the variational argument shows that for  $\varepsilon > 12$  there is a constant  $c^{(4)}$  such that in any ground-state the number  $|\mathcal{T}_{-,cb}(S)|$  of  $T$ -plaquette excitations is bounded from above as follows:

$$|\mathcal{T}_{-,cb}(S)| \leq \frac{c^{(4)} t^{-2}}{\varepsilon - 12} \sqrt{|\Lambda|}. \quad (21)$$

This means that, for  $0 < \rho_i < 1/2$  and sufficiently large lattice, any ground-state configuration of ions consists of connected regions whose ion configurations are restrictions to these regions of one of the configurations  $S_-$ ,  $S_{cb}^e$ ,  $S_{cb}^o$ . These connected regions are separated by domain walls that involve negligible, i.e.  $O(|\Lambda|^{-1/2})$  (for large lattice  $\Lambda$ ), fraction of sites.

Now, let us fix the ion density,  $\rho_i = 1/5$  or  $1/4$  or  $1/3$ , and a sufficiently small  $t$ . If we choose an initial value of  $\tilde{\varepsilon}$  so that  $\varepsilon = \tilde{\varepsilon}/t^4$  is greater than 12 (i.e. initially the system is in the state of phase-separation), then by decreasing  $\tilde{\varepsilon}$  sufficiently the system is driven into a crystalline state. But obviously, the same result can be arrived at, if we fix the value of  $\tilde{\varepsilon}$  and an (sufficiently small) initial value of  $t_0$  so that  $\varepsilon = \tilde{\varepsilon}/t_0^4 = 13$ , for instance, and then increase  $t$ . If not the fact that we have ignored the remainder  $R^{(4)}$  in the effective interaction, this would be the announced in the Introduction statement. Thus, it remains to be proven that the remainder  $R^{(4)}$  does not destroy the picture obtained with the truncated effective interaction  $E_S^{(4)}$ .

First, we shall demonstrate that if we take into account  $R^{(4)}$ , then there is a (sufficiently small) constant  $t_0$  such that for  $t < t_0$  the sets of ground-state

configurations of ions for densities  $\rho_i = 1/5, 1/4, 1/3$  coincide with the sets  $\mathcal{S}_1, \mathcal{S}_2$ , and  $\mathcal{S}_3$ , respectively. Specifically, we shall show that for  $t < t_0$  there are nonempty two-dimensional open domains  $\mathcal{S}_1^\infty, \mathcal{S}_2^\infty$ , and  $\mathcal{S}_3^\infty$  that are contained in the domains  $\mathcal{S}_1, \mathcal{S}_2$ , and  $\mathcal{S}_3$ , respectively, and such that in  $\mathcal{S}_j^\infty, j = 1, 2, 3$ , the set of ground-state configurations is  $\mathcal{S}_j$ . To achieve this we shall construct a lower bound for the energy difference  $E_S(0, -2t^2 + \delta t^4) - E_{S_j}(0, -2t^2 + \delta t^4)$ , with  $S_j \in \mathcal{S}_j$ . Clearly, we can restrict the set of all configurations  $S$  to those that do not contain any pairs  $\langle x, y \rangle_1$  with  $s_x = s_y = 1$ . With this restriction,

$$E_S(0, -2t^2 + \delta t^4) - E_{S_j}(0, -2t^2 + \delta t^4) = \frac{t^4}{2} \sum_{T \in \mathcal{T}_j(S)} \left[ (H_T^{(4)} + K_T^{(4)})|_S - (H_T^{(4)} + K_T^{(4)})|_{S_j} \right] + R^{(4)}|_S - R^{(4)}|_{S_j}. \quad (22)$$

Clearly,

$$\sum_{T \in \mathcal{T}_j(S)} \left[ (H_T^{(4)} + K_T^{(4)})|_S - (H_T^{(4)} + K_T^{(4)})|_{S_j} \right] \geq \tau_j |\mathcal{T}_j(S)| \quad (23)$$

where  $\mathcal{T}_j(S)$  is the set of  $T$ -plaquette excitations relative to the ground-state configurations from  $\mathcal{S}_j$  and

$$\tau_j = \min \left\{ (H_T^{(4)} + K_T^{(4)})|_S - (H_T^{(4)} + K_T^{(4)})|_{S_j} : S \notin \mathcal{S}_j \right\} \quad (24)$$

is a function of  $(\delta, \varepsilon)$  on the domain  $\mathcal{S}_j$ . Following [12] we have also the upper bound:

$$\left| R^{(4)}|_S - R^{(4)}|_{S_j} \right| \leq t^6 r_j |\mathcal{T}_j(S)| \quad (25)$$

for some constant  $r_j$ . From (22,23,25) we obtain

$$E_S(0, -2t^2 + \delta t^4) - E_{S_j}(0, -2t^2 + \delta t^4) \geq t^4 (\tau_j - r_j t^2) |\mathcal{T}_j(S)|. \quad (26)$$

Note that  $\mathcal{S}_j$  is an open convex domain in the  $(\delta, \varepsilon)$ -plane. For  $(\delta, \varepsilon) \in \mathcal{S}_j$ , the function  $(\delta, \varepsilon) \rightarrow \tau_j(\delta, \varepsilon)$ , being the minimum of a finite set of positive linear functions, is concave, piecewise linear and positive. It vanishes only at the boundary of  $\mathcal{S}_j$ . Therefore, there is a (sufficiently small)  $t_0$  such that for  $t < t_0$  the value of  $r_j t^2$  is less than the maximum of  $\tau_j$  over  $\mathcal{S}_j$ . Then, the level set  $\{(\delta, \varepsilon) : \tau_j(\delta, \varepsilon) > r_j t^2\}$  is a nonempty convex open set, contained in domain  $\mathcal{S}_j$ . At this level set the ground-state configurations coincide with the configurations from  $\mathcal{S}_j$ .

Second, we shall show that for a sufficiently small  $t$  the inequality (21) is modified by  $R^{(4)}$  only slightly, so that the conclusions drawn from (21) remain



valid. The remainder  $R^{(4)}$  can be estimated in the following way [16]:

$$\left| R^{(4)} \Big|_S - R^{(4)} \Big|_{S_-} - R^{(4)} \Big|_{S_{cb}} \right| \leq t^6 r_{-,cb} |\mathcal{T}_{-,cb}(S)|, \quad (27)$$

for some constant  $r_{-,cb}$ . Therefore, taking into account the remainder  $R^{(4)}$ , we replace the inequality (20) by

$$\begin{aligned} & \frac{t^4}{64} [\varepsilon - (12 + t^2 r_{-,cb})] |\mathcal{T}_{-,cb}(S)| \leq \\ & \frac{t^4}{2} \sum_T \left( H_T^{(4)} + K_T^{(4)} - E_T^{(-,cb)} \right) + \\ & t^2 \sum_{\substack{\langle x,y \rangle_1 \\ s_x=s_y=1}} 1 + R^{(4)} - R^{(4)} \Big|_{S_-} - R^{(4)} \Big|_{S_{cb}} \leq \mathcal{C} t^2 |\mathcal{T}_{-,cb}(S)|, \end{aligned} \quad (28)$$

for some constant  $\mathcal{C}$ . As a result, the variational argument of [16] implies that there is a constant  $c$  such that the following counterpart of (21) holds:

$$|\mathcal{T}_{-,cb}(S)| \leq \frac{ct^{-2}}{\varepsilon - (12 + 64r_{-,cb}t^2)} \sqrt{|\Lambda|}. \quad (29)$$

Consequently, for any density  $0 < \rho_i < 1/2$  and n.n.n. interaction  $\varepsilon > 12 + 64r_{-,cb}t^2$  the ground-state phase is a mixture of the  $\mathcal{S}_-$ -phase and  $\mathcal{S}_{cb}$ -phase.

Summing up, let the ion density be one of  $\rho_i = 1/5, 1/4$ , and  $1/3$ , and let the corresponding electron density be  $\rho_e = 1 - \rho_i$ . We restrict our considerations to the case  $\rho_i < 1/2$ , since the situation for  $\rho_i > 1/2$  can be obtained by means of symmetries (see subsection 2.1). Let the hopping intensity  $t$  be sufficiently small. Then, we have proved that the considered system can be driven from the state of phase separation (the mixture of  $\mathcal{S}_-$  and  $\mathcal{S}_{cb}$ -phases) to a crystalline state with a long-range order, which is the  $\mathcal{S}_j$ -phase whose particle densities are the chosen ones, by increasing quantum fluctuations (measured by  $t$ ) due to the hopping electrons.

Finally, it is easy to see that if the considered model is augmented by a n.n. repulsion between the ions, then the above analysis of the phase diagram can be carried out without any essential modifications. Thus, we arrive at the same conclusions concerning the transition from a state of phase separation to a state with a long-range order due to increasing hopping.

A similar discussion can be carried out in the case of hard-core bosons, with one exception. Our analysis shows that the transition from a state of phase separation to a state with a long-range order due to an increasing hopping occurs for densities  $\rho_i = 1/5, 1/3$ .

## Acknowledgements

It is a pleasure to thank Romuald Lemański for discussions. V.D. is grateful to the University of Wrocław, and especially to the Institute of Theoretical Physics for financial support.

## Appendix

Here we provide the tables of the coefficients  $\alpha_i$ ,  $i = 1, \dots, 5$ , of the zero-potentials in the case of hopping fermions and hopping hard-core bosons.

Table 1

Zero-potential coefficients  $\alpha_i$  for fermions ( $\varepsilon \geq 0$ )

	$\alpha_1$	$\alpha_2$	$\alpha_3$	$\alpha_4$	$\alpha_5$
$S_-, \varepsilon \leq 8$	0	$-\frac{\delta}{8}$	$\frac{\delta}{32} + \frac{1}{64}$	0	$-\frac{1}{48}$
$S_-, \varepsilon \geq 8$	0	$-\frac{\delta}{8}$	$\frac{\delta}{32} + \frac{\varepsilon}{128} - \frac{3}{64}$	0	$-\frac{1}{48}$
$S_1$	$-\frac{3\delta}{40} + \frac{\varepsilon}{160} - \frac{3}{80}$	$-\frac{\delta}{10} - \frac{\varepsilon}{80} + \frac{1}{80}$	0	$-\frac{\delta}{40} + \frac{\varepsilon}{80} - \frac{1}{80}$	$-\frac{1}{48}$
$S_2$	$-\frac{7\delta}{128} - \frac{\varepsilon}{256} - \frac{5}{64}$	$-\frac{9\delta}{64} + \frac{\varepsilon}{128} + \frac{3}{32}$	0	$\frac{\delta}{128} - \frac{\varepsilon}{256} - \frac{5}{64}$	$\frac{\delta}{128} - \frac{\varepsilon}{256} - \frac{7}{192}$
$S_3, \varepsilon \leq 4$	$-\frac{11\delta}{144} - \frac{\varepsilon}{144} + \frac{5}{96}$	$-\frac{\delta}{8}$	0	$\frac{\delta}{144} + \frac{\varepsilon}{288} - \frac{7}{96}$	$-\frac{\delta}{144} - \frac{\varepsilon}{288} + \frac{5}{96}$
$S_3, 4 \leq \varepsilon \leq 8$	$-\frac{\delta}{12} - \frac{\varepsilon}{384} + \frac{1}{16}$	$-\frac{\delta}{8}$	0	$\frac{\varepsilon}{128} - \frac{1}{16}$	$-\frac{\varepsilon}{128} + \frac{1}{24}$
$S_3, \varepsilon \geq 8$	$-\frac{\delta}{12} - \frac{\varepsilon}{96} + \frac{1}{8}$	$-\frac{\delta}{8}$	0	0	$-\frac{1}{48}$
$S_{cb}$	0	$-\frac{\delta}{8}$	$\frac{185\delta}{5856} + \frac{\varepsilon}{5856} + \frac{169}{3904}$	0	$-\frac{1}{48}$

Table 2

Zero-potential coefficients  $\alpha_i$  for hard-core bosons ( $\varepsilon \geq -4$ )

	$\alpha_1$	$\alpha_2$	$\alpha_3$	$\alpha_4$	$\alpha_5$
$S_-, \varepsilon \leq 4$	0	$-\frac{\delta}{8}$	$\frac{\delta}{32} - \frac{1}{192}$	0	$-\frac{1}{48}$
$S_-, \varepsilon \geq 4$	0	$-\frac{\delta}{8}$	$\frac{\delta}{32} + \frac{\varepsilon}{128} - \frac{7}{192}$	0	$-\frac{1}{48}$
$S_1$	$-\frac{3\delta}{40} + \frac{\varepsilon}{160} + \frac{1}{240}$	$-\frac{\delta}{10} - \frac{\varepsilon}{80} + \frac{1}{80}$	0	$-\frac{\delta}{40} + \frac{\varepsilon}{80} - \frac{1}{80}$	$-\frac{1}{48}$
$S_2$	$-\frac{7\delta}{128} - \frac{\varepsilon}{256} - \frac{7}{192}$	$-\frac{9\delta}{64} + \frac{\varepsilon}{128} + \frac{3}{32}$	0	$\frac{\delta}{128} - \frac{\varepsilon}{256} - \frac{5}{64}$	$\frac{\delta}{128} - \frac{\varepsilon}{256} - \frac{7}{192}$
$S_3, \varepsilon \leq 0$	$-\frac{11\delta}{144} - \frac{\varepsilon}{144} + \frac{11}{288}$	$-\frac{\delta}{8}$	0	$\frac{\delta}{144} + \frac{\varepsilon}{288} - \frac{13}{288}$	$-\frac{\delta}{144} - \frac{\varepsilon}{288} + \frac{7}{288}$
$S_3, 0 \leq \varepsilon \leq 4$	$-\frac{\delta}{12} - \frac{\varepsilon}{384} + \frac{5}{96}$	$-\frac{\delta}{8}$	0	$\frac{\varepsilon}{128} - \frac{1}{32}$	$-\frac{\varepsilon}{128} + \frac{1}{96}$
$S_3, \varepsilon \geq 4$	$-\frac{\delta}{12} - \frac{\varepsilon}{96} + \frac{1}{12}$	$-\frac{\delta}{8}$	0	0	$-\frac{1}{48}$
$S_{cb}$	0	$-\frac{\delta}{8}$	$\frac{185\delta}{5856} + \frac{\varepsilon}{5856} + \frac{93}{3904}$	0	$-\frac{1}{48}$

## References

- [1] M. Nakamura, *Tricritical behaviour in the extended Hubbard chains*, Phys. Rev. B **61**, 16377 (2000).

- [2] P. Sengupta, A. W. Sandvik, and D. K. Campbell, *Bond-order-wave phase and quantum phase transitions in the one-dimensional extended Hubbard model*, Phys. Rev. B **65**, 155113 (2002).
- [3] E. Jeckelmann, *Ground-state phase diagram of a half-filled one-dimensional extended Hubbard model*, Phys. Rev. Lett. **89**, 236401 (2002).
- [4] A. W. Sandvik, P. Sengupta, and D. K. Campbell, *Comment on "Ground state phase diagram of a half-filled one-dimensional extended Hubbard model"*, arXiv:cond-mat/0301237
- [5] L. M. Falicov and J. C. Kimball, *Simple model for semiconductor-metal transitions:  $\text{SmB}_6$  and transition-metal oxides*, Phys. Rev. Lett. **22**, 997 (1969).
- [6] U. Brandt, R. Schmidt, *Exact results for the distribution of the  $f$ -level ground state occupation in the spinless Falicov–Kimball model*, Z. Phys. B **63**, 45 (1986).
- [7] T. Kennedy and E. H. Lieb, *An itinerant electron model with crystalline or magnetic long range order*, Physica A **138**, 320 (1986).
- [8] C. Gruber and N. Macris, *The Falicov–Kimball model: a review of exact results and extensions*, Helv. Phys. Acta **69**, 850 (1996).
- [9] J. Jędrzejewski and R. Lemański, *Falicov–Kimball models of collective phenomena in solids (a concise guide)*, Acta Phys. Pol. B **32**, 3243 (2001).
- [10] C. Gruber, J. Jędrzejewski and P. Lemberger, *Ground states of the spinless Falicov–Kimball model. II*, J. Stat. Phys. **66**, 913 (1992).
- [11] T. Kennedy, *Some rigorous results on the ground states of the Falicov–Kimball model*, Rev. Math. Phys. **6**, 901 (1994).
- [12] C. Gruber, N. Macris, A. Messenger and D. Ueltschi, *Groundstates and flux configurations of the two-dimensional Falicov–Kimball model*, J. Stat. Phys. **86**, 57 (1997).
- [13] J. Slawny, *Low-temperature properties of classical lattice systems: phase transitions and phase diagrams*, In: *Phase Transitions and Critical Phenomena* vol. **11**, C. Domb and J. Lebowitz, eds (Academic Press, London/New York 1985).
- [14] J. Fröhlich, R.B. Israel, E.H. Lieb and B. Simon, *Phase transitions and reflection positivity. II. Lattice systems with short-range and Coulomb interactions*, J. Stat. Phys. **22**, 297 (1980).
- [15] G.I. Watson, *Repulsive particles on a two-dimensional lattice*, Physica A **246**, 253 (1997).
- [16] T. Kennedy, *Phase separation in the neutral Falicov-Kimball model*, J. Stat. Phys. **91**, 829 (1998).